J. Biochem. 2011;149(2):203–210 doi:10.1093/jb/mvq130

JB THE JOURNAL OF BIOCHEMISTRY

Interaction defect of the medium isoform of PTS1-receptor Pex5p with PTS2-receptor Pex7p abrogates the PTS2 protein import into peroxisomes in mammals

Received September 11, 2010; accepted October 28, 2010; published online November 2, 2010

Masanori Honsho[1], Yasuko Hashiguchi[1], Kamran Ghaedi[1,*] and Yukio Fujiki[1,2,†]

[1]Department of Biology, Faculty of Sciences, Kyushu University Graduate School, 6-10-1 Hakozaki, Higashi-ku, Fukuoka 812-8581 and [2]CREST, Japan Science and Technology Agency, Chiyoda, Tokyo 102-0075, Japan

*Present address: Department of Biology, School of Sciences, University of Isfahan, Isfahan; Cell & Molecular Biology Department, Royan Institute for Animal Biotechnology, ACECR, Isfahan, 81746-73441, Iran

†Dr. Yukio Fujiki, Department of Biology, Faulty of Sciences, Kyushu University Graduate School, 6-10-1 Hakozaki, Higashi-ku, Fukuoka 812-8581, Japan. Tel: +81 092 642 2635, Fax: +81 092 642 4214, email: yfujiki@kyudai.jp

We earlier isolated peroxisome biogenesis-defective Chinese hamster ovary (CHO) cell mutants, ZPEG241, by the 9-(1′-pyrene)nonanol/ultraviolet selection method, from TKaEG2, the wild-type CHO-K1 cells transformed with two cDNAs encoding rat Pex2p and peroxisome targeting signal type 2 (PTS2)-tagged enhanced green fluorescent protein (EGFP). Peroxisomal localization of PTS2-EGFP was specifically impaired in ZPEG241 due to the failure of Pex5pL expression. Analysis of partial genomic sequence of *PEX5* revealed one-point nucleotide-mutation from G to A in the 3′-acceptor splice site located at 1 nt upstream of exon 7 encoding Pex5pL specific 37-amino acid insertion, thereby generating 21-nt deleted mRNA of *PEX5L* in ZPEG241. When ZPEG241-derived Pex5pL was ectopically expressed in ZPEG241, PTS2 import was not restored because of no interaction with Pex7p. Together, we confirm the pivotal role of Pex5pL in PTS2 import, showing that the N-terminal 7-amino acid residues in the 37-amino acid insertion of Pex5pL are essential for the binding to Pex7p.

Keywords: CHO cell mutants/peroxisome biogenesis/peroxin splicing variants/protein import/PTS1 receptor.

Abbreviations: ADAPS, alkyl-dihydroxyacetonephosphate synthase; AOx, acyl-CoA oxidase; CHO, Chinese hamster ovary; EGFP, enhanced green fluorescent protein; HA, influenza virus haemagglutinin; Pex5pS and Pex5pL, a shorter and a longer isoforms of Pex5p; PTS1 and PTS2, peroxisome targeting signal types 1 and 2; RT, reverse transcription; thiolase, peroxisomal 3-ketoacyl-CoA thiolase; 4-PB, 4-phenylbutyrate.

Cell mutants with genetic defects affecting biological activities are a highly useful tool in genetic, biochemical and cell biology research. To investigate peroxisome biogenesis and human peroxisome biogenesis disorders, more than 15 different complementation groups of Chinese hamster ovary (CHO) cell mutants defective in peroxisome assembly have been successfully isolated by the combination of 9-(1′-pyrene) nonanol (P9OH/UV) selection and monitoring the localization of peroxisomal matrix proteins using peroxisome targeting signal (PTS)-tagged enhanced green fluorescent protein (EGFP) (*1*).

Peroxisomal matrix proteins are synthesized on free polysomes in cytoplasm (*2*) and transported into peroxisomes in a manner dependent on PTS. Two types of PTS, PTS1 and PTS2, of matrix proteins have been identified (*3*). PTS1 consists of the tripeptide SKL motif found in the C-terminal of most of peroxisomal matrix proteins. PTS2 consists of N-terminal cleavable presequence containing a nonapeptide with the conserved sequence, $(R/K)(L/V/I)X_5(H/Q)(L/A)$. PTS1 and PTS2 are recognized by their cytosolic receptors, Pex5p and Pex7p, respectively. In mammals, two types of Pex5p are identified: shorter and longer forms of Pex5p, termed Pex5pS and Pex5pL, respectively (*4*). Pex5p acts as a PTS1 receptor and transports its cargo proteins to peroxisomes by binding to the membrane receptor, Pex14p (*5*). In the import of PTS2-proteins, Pex5pL functions in the transport to peroxisomes of not only PTS1-cargoes but also Pex7p-PTS2-protein complexes (*5*). Exclusive requirement of Pex5pL for the transport of PTS2-proteins is evidently demonstrated with a *pex5* CHO cell mutant, ZPG231, where the impaired PTS2-protein import is restored only by Pex5pL (*6*).

Recently, we isolated another *pex5* CHO mutant ZPEG241 showing the same phenotype as ZPG231, where the impaired PTS2-protein import was likewise restored by the expression of *PEX5L* (*7*). We herein further analyse the phenotype and its genetic cause of ZPEG241.

Experimental Procedures

Cell culture and DNA transfection

CHO cells, including wild-type CHO-K1, TkaEG2 (*8*), ZPEG241 (*9*) and ZP105 (*4*), were cultured as described (*10*, *11*). Transfection of *PEX5* cDNAs to CHO mutant cells was done by lipofection as described (*12*).

Morphological analysis

Peroxisomes in CHO cells were visualized by indirect immunofluorescence light microscopy using rabbit antibodies to PTS1 peptide (*4*) and catalase (*10*) and mouse antibody to influenza virus

haemagglutinin (HA) (16B2, Covance). Antigen-antibody complex was detected by Alexa 568- and 633-labelled goat anti-rabbit or mouse antibody (Invitrogen) (*13*), under a confocal microscope (LSM 510; Carl Zeiss).

Subcellular fractionation

A post-nuclear supernatant fraction was prepared from cell homogenates of TkaEG2 and ZPEG241 (*14*). Organelle and cytosol fractions were prepared from the post-nuclear supernatant fraction as described (*5*). Subcellular fractions and total cell lysates were analysed by SDS–PAGE and immunoblot with specific antibodies against Pex14p (*15*), catalase (*10*), lactate dehydrogenase (LDH) (*16*), actin (*17*), alkyl-dihydroxyacetonephosphate synthase (ADAPS) (*14*), 3-ketoacyl-CoA thiolase (thiolase) (*10*) and Pex5p (*5*).

Reverse transcription–PCR

Total RNA was prepared from TKaEG2 and ZPEG241 using a FastPureTM RNA kit (Takara) according to the manufacturer's instruction. The first strand cDNA was obtained by reverse transcription (RT) using the total RNA (0.5 μg). The entire open reading frame of *PEX5* was amplified using a set of primers, a sense 59F: 5′-AGCTGGTGGTCACCATGGCAATGAG-3′ and an anti-sense 2043R: 5′-TGGAGGAGAGGGAGTCACATCCAG A-3′. Resulting *PEX5* cDNA was cloned into T-easy vector (Promega) and its nucleotide sequence was determined from three independent clones. To analyse the expression of *PEX5* isoforms, a sense 488F: 5′-ATCTGGAGCAGTCTGAGGAGAAGC-3′ and an anti-sense 676R: 5′-GTGAACTGATCGACCCAGGCCTCTG-3′ were used. PCR products were analysed 2.5% agarose gel electrophoresis using Certified LowRange Ultra agarose (Bio-Rad). Transcriptional level of *PEX5* isoforms in TkaEG2, ZPEG241 and CHO-K1 was assessed by PCR as follows. A partial cDNA of *PEX5* was amplified with a pair of primers 488F and 941R: 5′-AAAAAGC AGCACGGCATTGGGCAG-3′. Resulting PCR product was used as a template for the second PCR. To amplify *PEX5L* and *PEX5S* isoforms, a pair of primers 645F: 5′-GTTCCTGAAATTCGTGCG ACA-3′ and 879R: 5′-TTTGCCATCTCCTCCAACTCTGCC-3′ and another pair of primers 624F: 5′-CCCCAAATTGGCTAACT CCGGGGCA-3′ and 879R were respectively used. Transcriptional levels of *PEX5* isoforms in human cell lines: HeLa, HEK293 and fibroblasts from a normal control, mouse Neuro 2a, rat C6 glioma and rat Fao cells were likewise analysed using species-specific primers synthesized at the same alignment positions as the CHO sequences.

PEX5L isoform was also amplified using as a template the RT products from total RNA of CHO cells (see above) with a set of primers 645F and 879R (Fig. 3A). *AOx*, *GAPDH* encoding -glyceraldehyde-3-phosphate dehydrogenase, and *PEX7* were PCR-amplified with respective pairs of primers: AOx.Fw 5′-ACAA GCTGACGTATGGGACC-3′ and AOx.Rv 5′-CTGGTTCACCTG GCTTGATT-3′; GAPDH.Fw 5′-CGGTATTGGACGCCTGGT TA-3′ and GAPDH.Rv 5′-TGGCAACAACTTCCACTTTGC-3′; *Cl*PEX7.Fw: 5′-TCTGGGACACTGCCAAAGC-3′ and *Cl*PEX7.Rv: 5′-ACACCTCCTGAGTGTGTTCTTTATAGA-3′. CHO-K1 cells were cultured for 3 days in the presence or absence of 5 mM 4-phenylbutyrate (4-PB) (Wako Chemicals, Osaka, Japan). Expression levels of these genes after 4-PB treatment was analysed by RT–PCR using different concentration of the first strand as a template. We confirmed that PCR products of respective genes were within the range of linearity.

Genome sequencing

Partial genomes each of TkaEG2- and ZPEG241-derived *PEX5* were amplified using a pair of primers designed with mouse genome sequence encompassing ~90 bp of 3′-side of intron 6 and ~90 bp of 5′-side of exon 7, a forward 557F: 5′-ATGATGACTATCATCC CGAGGAGGATCTGC-3′ and a reverse 730R: 5′-GCTGACTTG GCTCGTTCAAATTCTACATCC-3′. The amplified fragments were cloned into T-easy vector (Promega) and determined for their sequence of three each independent clones.

Pex7p–Pex5p interaction assay

Expression plasmids for cDNAs encoding Pex5pL and Pex5pS, both tagged with hexa-His (His) and HA at the N- and C-terminus, respectively, were constructed in pcDNA3.1Zeo (K. Okumoto and Y. Fujiki, unpublished reults), termed pcDNA3.1Zeo*His-PEX5L-HA* and His-*PEX5S*-HA, respectively. For epitope tagging of ZPEG241-derived *PEX5*, 24 nt longer *PEX5L**, and *PEX5S**, respective *PEX5* isoforms in T-easy vector were digested with Sse8387I and AxyI and cloned into the Sse8387I-AxyI site of pcDNA3.1Zeo*His-ClPEX5S-HA*. These *PEX5* expressing vectors and pcDNA3.1Zeo*Flag-PEX7* (*18*) were transfected into ZPEG241 cells. From cell lysates (*19*), Flag-Pex7p was immunoprecipitated at 4°C using agarose beads conjugated with anti-Flag antibody (M2, Sigma).

Results

Morphological and biochemical characterization of ZPEG241

To elucidate molecular mechanism of peroxisome biogenesis, we previously isolated ZPEG241 from TKaEG2, CHO-K1 cells stably expressing Pex2p and PTS2-EGFP (*7*). In ZPEG241 PTS2-EGFP was discernible in a diffused pattern in contrast to numerous punctate signals, peroxisomes, in TKaEG2 (Fig. 1A, a, b, e and f). When ZPEG241 was stained with antibodies to PTS1 and catalase, a punctate staining pattern was observed (Fig. 1A, d and h), as in TKaEG2 (c and g). We next verified the biogenesis of peroxisomal enzymes by immunoblotting. Acyl-CoA oxidase (AOx) comprises 75-kDa A, 53-kDa B and 22-kDa C polypeptide components; B and C are derived from A by proteolytic conversion in peroxisomes (*10*, *20*). All of three components were evident in ZPEG241 at the same level as in TkaEG2 (Fig. 1B, middle panel), indicative of normal biogenesis of AOx and consistent with the morphological observation of PTS1-proteins. Peroxisomal thiolase and ADAPS are synthesized as a larger precursor and then converted to mature form by PTS2 cleavage in peroxisomes (*10*, *14*, *21*). In ZPEG241, precursor forms of 44-kDa thiolase and 72-kDa ADAPS were observed, whereas mature forms of respective enzymes were apparent in TKaEG2 (Fig. 1B, upper two panels). Collectively, we interpret these results to mean that PTS2-protein import is specifically impaired in ZPEG241.

Dysfunction of Pex5p in ZPEG241

Upon expression of *PEX5L* in ZPEG241, the compromised peroxisomal import of PTS2-EGFP was restored (Fig. 2A, c and d), while *PEX5S* expression did not rescue the defect (a and b). These results suggested that dysfunction of *PEX5L* is responsible for the defect of PTS2-protein import in ZPEG241.

To investigate whether the impaired function of Pex5pL in ZPEG241 is caused by genetic defect of *PEX5L*, we performed RT–PCR using total RNA and *PEX5*-specific primers. A deletion of 21-bp sequence corresponding to the N-terminal 7-amino acid residues, -FLKFVRQ-, of the Pex5pL-specific 37-amino acid insertion encoded by one 111-bp exon (*4*) was found in all of three cDNA clones isolated (Fig. 2B, lower left panel). Next, we performed RT–PCR to amplify the region including the sequence coding for the 37-amino acid insertion. In TkaEG2 cells, 301- and 190-bp PCR products corresponding to this region of *PEX5L* and *PEX5S* were detected (Fig. 2B, upper panel, lanes 1, 3 and 4; solid and

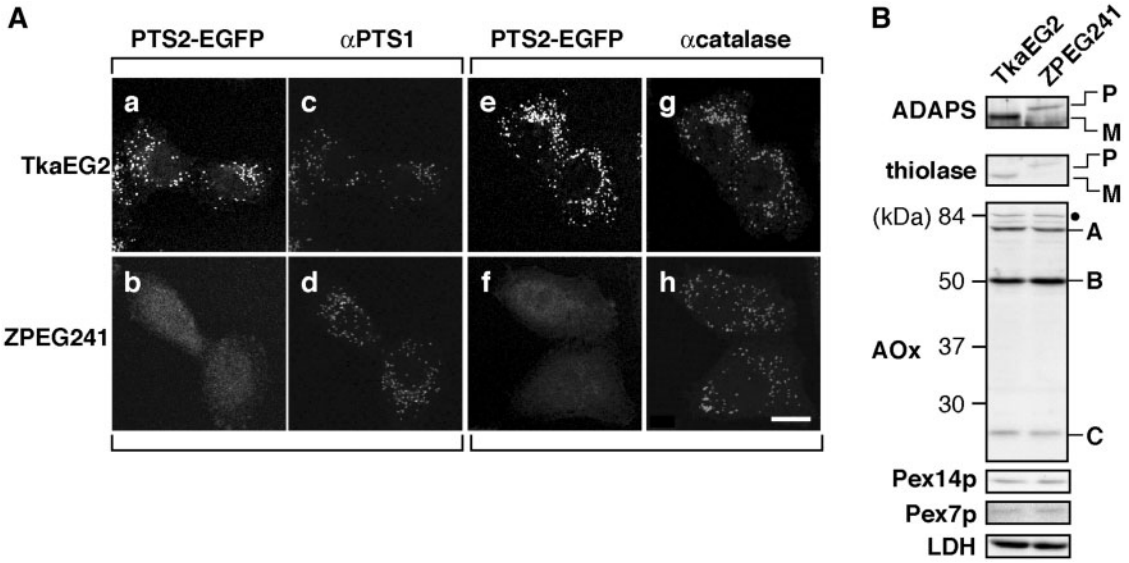

Fig. 1 Characterization of peroxisome biogenesis-defective CHO cell mutant ZPEG241. (A) Wild-type TKaEG2 (*9*) (upper panels), rat *PEX2*-transformed wild-type CHO-K1 stably expressing PTS2-GFP, and ZPEG241 isolated from TKaEG2 (lower panels) were fixed and dually monitored for GFP fluorescence (a, b, e and f) and by immunofluorescent staining with antibodies to PTS1 (c and d) and catalase (g and h), using fluorescence microscopy. TKaEG2 and ZPEG241 were respectively pair-wise verified: a and c plus e and g, TKaEG2; b and d plus f and h, ZPEG241. Scale, 5 μm. Note that ZPEG241 is defective only in PTS2 import. (B) Biosynthesis of peroxisomal enzymes. Cell lysates (3×10^6 each) were subjected to SDS–PAGE and transferred to polyvinylidene difluoride membrane. Immunoblot analysis was performed with antibodies to ADAPS, thiolase, AOx, Pex14p, Pex7p and LDH. Full-length AOx-A chain is converted to B- and C-chains in peroxisomes (*10*, *20*). P, a larger precursor; M, mature protein. Dot indicates a non-specific band.

open arrowheads). In RT–PCR products using ZPEG241-derived RNA, a band with mobility apparently equivalent to the amplified region of *PEX5S* was detected (Fig. 2B, upper panel, lane 5; open arrowhead). In contrast, any RT–PCR product corresponding to the amplified region of *PEX5L* was hardly detectable from ZPEG241, but a rather slightly higher-mobility band was discernible at a lower level (Fig. 2B, upper panel, lane 5; shaded arrowhead). To delineate how such a *PEX5* transcript is generated in ZPEG241, we determined nucleotide sequence of a part of *PEX5* gene. Partial, ~180 bp-long genome of *PEX5* from TKaEG2 and ZPEG241 was amplified with a set of primers designed using the mouse genome sequence as described in Experimental Procedures. By subsequent sequencing of three each independent clones from TkaEG2 and ZPEG241, we identified in ZPEG241-derived PCR product harboring a point mutation of nucleotide G to A, commonly at 3′-end splice-acceptor site locating at 1 nt upstream of putative exon 7 encoding Pex5pL-specific 37-amino acid insertion (Fig. 2B, lower right panel, red arrow). We interpreted this finding to mean that the failure in splicing at the junction of intron 6 and exon 7 owing to the G-to-A mutation resulted in abnormal splicing at G at nucleotide position 21 in the exon 7, thereby inducing a 21-bp shorter *PEX5L* open reading frame.

We also assessed the expression of Pex5 proteins by immunoblotting (Fig. 2C). As inferred from the RT–PCR results, Pex5pS was detected at the same level in both ZPEG241 and TkaEG2. In contrast, any other Pex5 proteins were barely detectable in ZPEG241, whereas Pex5pL was discernible in TkaEG2, confirming that Pex5pL was not expressed in ZPEG241. It is noteworthy that $Pex5p_{ZPEG241}$ is not discernible in the immunoblot of ZPEG241 (Fig. 2C). Furthermore, to verify whether $Pex5p_{ZPEG241}$ is functional, *PEX5L*, $PEX5_{ZPEG241}$ and *PEX5S* were separately transfected to ZPEG241. $Pex5p_{ZPEG241}$ was expressed as efficiently as Pex5pL and Pex5pS in ZPEG241 under the transient expression condition (Fig. 2D, lanes 3–5). However, $Pex5p_{ZPEG241}$ as well as Pex5pS did not restore the defect of PTS2-EGFP import (Fig. 2A, left panels; Fig. 2D, right panels) and the compromised processing of ADAPS precursor, while Pex5pL was fully functional (Fig. 2D, lanes 3–5, upper panel). Taken together, these results strongly suggested that Pex5pL expression is impaired by abnormal splicing caused by the point mutation at the acceptor site of the intron 6.

PEX5 isoforms and their function

We earlier screened a cDNA library of CHO-K1 cells with human full-length *PEX5* cDNA as a probe and isolated Chinese hamster *PEX5S* and *PEX5L* encoding Pex5pS and Pex5pL comprising 595 and 632 amino acid residues, respectively (*4*). These *PEX5S* and *PEX5L* expression efficiently restored the impaired protein import in *pex5* mutants: Pex5pS and Pex5pL re-established PTS1-protein import and Pex5pL did PTS2-protein import in *pex5* ZP105 (*4*). Pex5pL restores the compromised PTS2-protein import in *pex5* ZPG231 with a phenotype of normal PTS1 import (*6*). Eight amino acid longer forms of Pex5pS and Pex5pL were also identified (*22*). Therefore, in the present study we also verified the expression level of respective *PEX5* isoforms by RT–PCR and assessed their biological activities in peroxisomal matrix protein

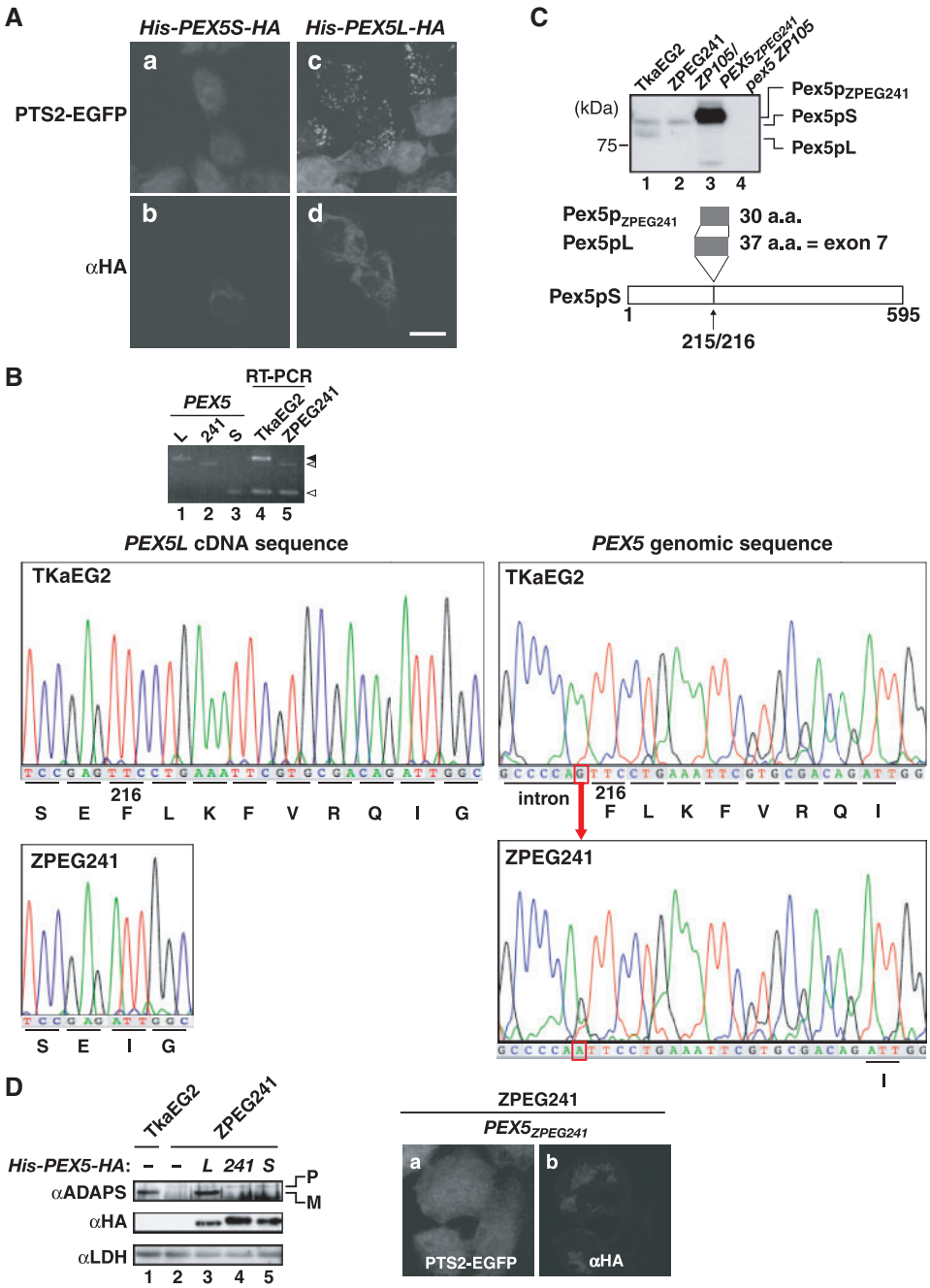

Fig. 2 Expression of Pex5pL is impaired in ZPEG241. (A) ZPEG241 was transfected with *His-PEX5S-HA* and *His-PEX5L-HA*, and was verified for peroxisomal import of PTS2-EGFP (a and c). Expression of Pex5p isoform was assessed by staining with anti-HA antibody (b and d). Scale, 5 μm. (B) Mutation analysis of *PEX5* in ZPEG241. RT–PCR was performed with primers to amplify the nucleotide residues at positions 488–788 of *PEX5* including the region encoding Pex5L-specific 37 amino acid insertion. Amplified DNA products were analysed by agarose gel electrophoresis (upper panel). Cell types were indicated at the top (lanes 4 and 5). PCR products amplified from the plasmid encoding *PEX5L*, $PEX5_{ZPEG241}$ and *PEX5S* were used as a positive control (lanes 1–3). Note that a DNA fragment with slightly higher migration (upper panel, lane 5, shaded arrowhead) but not for *PEX5L* was detectable in ZPEG241, in contrast to *PEX5S* and *PEX5L* in TKaEG2 (upper panel, lane 4, open and solid arrowheads). Nucleotide sequences of *PEX5L* cDNA (middle and lower left panels) and the region encompassing intron 6 and exon 7 of *PEX5* genes (middle and lower right panels) from wild-type TKaEG2 and ZPEG241 were determined. A point mutation at nucleotide residue G to A in the 3′-splicing accepter site in the intron 6 was detected (lower panels). This mutation resulted in the failure in splicing at the junction of intron 6 and exon 7, inducing a splicing at G in exon 7, 21-base downstream of the authentic G. (C) Expression of endogenous Pex5p was verified by immunoblot. Upper panel, in ZPEG241, only Pex5pS was detectable (lane 2). *pex5* CHO mutant ZP105 (lane 4) was transfected with $PEX5_{ZPEG241}$ (lane 3). $Pex5p_{ZPEG241}$ migrated with mobility lower than Pex5pS in SDS–PAGE. Lower panel, a schematic view of three distinct Pex5p in CHO cells is shown. (D) Left panel, three isoforms of Chinese hamster *PEX5*, including *His-PEX5L-HA*, *His-*$PEX5_{ZPEG241}$*-HA* and *His-PEX5S-HA*, were separately transfected into ZPEG241. Restoration of PTS2-protein import was assessed by monitoring proteolytic processing of ADAPS. His-Pex5p-HA variants were detected by immunoblotting with anti-HA antibody. LDH was used for a loading control. Lanes: 1 and 2, mock-transfected TKaEG2 and ZPEG241; 3-5, ZPEG241 cells transfected with *PEX5* variants. Note that only *PEX5L* expression restored the processing of ADAPS. Right panel, $PEX5_{ZPEG241}$ was verified for PEX5L-specifc complementing activity in restoring the impaired PTS2 import in ZPEG241. ZPEG241 was transfected with *His-*$PEX5_{ZPEG241}$*-HA* and assessed for peroxisomal import of PTS2-EGFP.

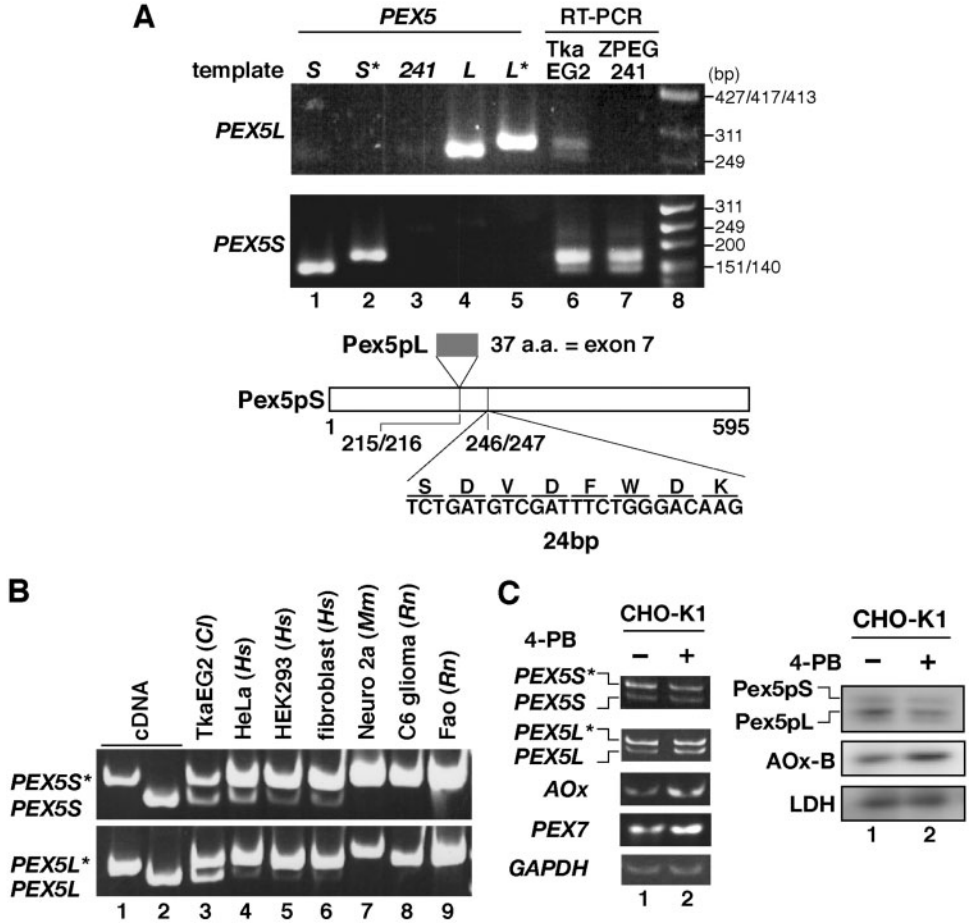

Fig. 3 Expression level of *PEX5* splicing variants. (A) Transcriptional level of *PEX5* isoforms, *PEX5L* and *PEX5S*. *PEX5L* (upper panel) and *PEX5S* (middle panel) isoforms were amplified as described in 'Experimental Procedures' section. Specific amplification of *PEX5* isoforms was confirmed with cloned cDNA as a template. *L* and *S* represent *PEX5L* and *PEX5S* and *L** and *S** designate 24 nt longer isoforms of *PEX5L* and *PEX5S*, respectively. Lanes: 1–5, PCR products with cloned *PEX5* variants; 6 and 7, RT–PCR products using total RNA from TKaEG2 and ZPEG241 cells; 8, DNA size markers in base pair (bp). Insertion of 24 nt into *PEX5* is illustrated (lower panel). (B) Expression of *PEX5* isoforms in various mammalian cell lines. *Cl*, Chinese hamster; *Hs*, human; *Mm*, mouse; *Rn*, rat. *PEX5* isoforms were amplified using total RNA from each cell line with a set of primers for respective isoforms as described in Experimental Procedures and analysed by 12% polyacrylamide gel. PCR products amplified from the plasmids each for four *PEX5* isoforms of CHO-K1 cells were used as a positive control (lanes 1 and 2). (C) Treatment with a peroxisome proliferator, 4-PB. CHO-K1 cells were cultured for 3 days in the presence (+, lane 2) or absence (–, lane 1) of 5 mM 4-PB. Left panels, transcriptional level of *PEX5* isoforms, *AOx*, *PEX7* and *GAPDH* for glyceraldehyde-3-phosphate dehydrogenase was verified by RT–PCR. Right panels, expression level of Pex5pL, Pex5pS, AOx, and LDH was assessed with antibodies to respective proteins.

transport. Two RT–PCR products of *PEX5L* were obtained from the parental cell, TkaEG2 (Fig. 3A, upper panel, lane 6), respectively showing the same migration as the cloned *PEX5L* and 24 nt longer *PEX5L** (lanes 4 and 5). RT–PCR for *PEX5S* likewise gave rise to two distinct bands apparently comigrating with the cloned *PEX5S* and 24 nt longer *PEX5S** (Fig. 3A, middle panel, lanes 1, 2 and 6), hence confirming that another type of isoforms, *PEX5L**and *PEX5S**, were transcribed in CHO-K1 cells.

We verified expression of *PEX5* isoforms by RT–PCR in various mammalian cell lines. *PEX5L** and *PEX5S**, 24 nt longer form of *PEX5L* and *PEX5S*, were predominantly expressed in Chinese hamster, human, mouse and rat cell lines (Fig. 3B). In contrast, *PEX5L* and *PEX5S* were distinctly transcribed but at a lower level only in Chinese hamster and human cell lines including HeLa and HEK293 (Fig. 3B, lanes 3–6). We further investigated whether *PEX5* isoforms are altered at their transcriptional level upon treatment of cells with a peroxisome proliferator, 4-PB (*23*). Transcriptional level of *AOx* and *PEX7* was significantly elevated in CHO-K1 cells cultured in the presence of 4-PB (Fig. 3C, left panels), consistent with the findings in the liver of rats treated with clofibrate, a hypolipidemic drug (*24*). However, *PEX5* isoforms were not induced at their transcriptional level under such conditions (Fig. 3C, left panels). Induction of AOx, but not Pex5p isoforms, was confirmed by immunoblotting of 4-PB-treated CHO-K1 cells (Fig. 3C, right panels).

Next, we assessed the potency of Pex5p isoform by expressing respective *PEX5* cDNAs in *pex5* ZP105 cells. All of Pex5p variants restored the impaired biogenesis of AOx as verified as the appearance of AOx-A converted form, AOx-B in *pex5* ZP105 (Fig. 4A). Furthermore, we investigated the interaction of respective Pex5p isoforms with Pex7p. Each of Pex5p

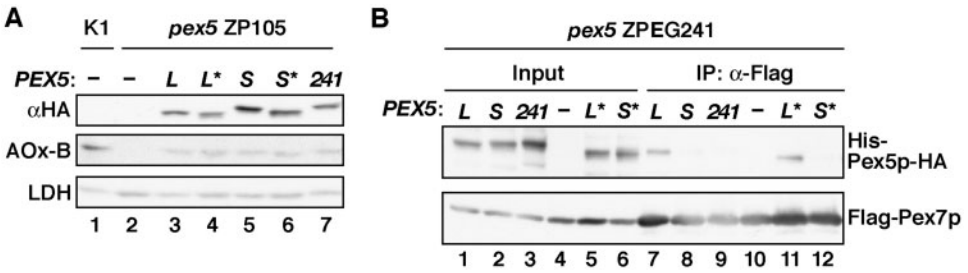

Fig. 4 Distinct biological activities of Pex5p isoforms. (A) PTS1-protein import activity of Pex5p isoforms in *pex5* ZP105. *His-PEX5-HA* isoforms, including *PEX5L* (*L*), *L**, *PEX5S* (*S*), *S** and $PEX5_{ZPEG241}$, were separately transfected into *pex5* ZP105, and were assessed for their PTS1-protein import activity by monitoring AOx conversion. Only AOx-B chain was shown. His-Pex5p-HA isoforms were detected by immunoblotting with anti-HA antibody. LDH was used for a loading control. *B*, ZPEG241-derived Pex5p fails to interact with Pex7p. Five *His-PEX5-HA* isoforms, *L*, *L**, *S*, *S** and $PEX5_{ZPEG241}$ were separately co-transfected with *Flag-PEX7* to ZPEG241. Flag-Pex7p was immunoprecipitated from respective cell-lysates with anti-Flag antibody conjugated to agarose beads. Immunoprecipitates were assessed for His-Pex5p-HA and Flag-Pex7p by immunoblotting with antibodies to HA and Flag, respectively (lanes 7–12). One-fortieth aliquots were loaded as an input (lanes 1–6). Note that Flag-Pex7p bound only to Pex5pL and Pex5pL*.

isoforms and Flag-tagged Pex7p were co-expressed in ZPEG241 cells. In Flag-Pex7p immunoprecipitates, only Pex5pL and Pex5pL*, not $Pex5p_{ZPEG241}$, Pex5pS and Pex5pS*, were detected (Fig. 4B), hence indicating that Pex5pL and Pex5pL* bound to Pex7p. Taken these results together, we conclude that the first 7 amino acid residues of 37-amino acid insertion in Pex5pL are critical for the binding to Pex7p.

Discussion

Deficiency in PTS2 transport is a characteristic of *pex7* mutants caused by dysfunction of the PTS2 receptor, Pex7p (*25*, *26*), not only in yeast (*27*, *28*) but also in mammalian cells such as fibroblasts from patients with RCDP (*29–31*) and CHO cell mutant (*24*). The exclusively importance of Pex5pL in the PTS2 pathway is highlighted by the study of the CHO mutant, ZPG231, showing specific impairment of PTS2 pathway caused by the S214F mutation in the Pex7p-binding region of Pex5pL (*6*). Interestingly, PTS2 pathway was specifically impaired in ZPEG241 due to the complete elimination of Pex5pL expression, confirming the pivotal role of Pex5pL in the PTS2 pathway. At any event, $Pex5p_{ZPEG241}$ is not potent in binding to Pex7p even when $Pex5p_{ZPEG241}$ is highly expressed in ZPEG241 cells, evidently being responsible for the ZPEG241 phenotype.

In the mutation analysis of ZPEG241, we found that 21 nt shorter form of *PEX5L* was transcribed in ZPEG241, presumably due to the newly generated acceptor splice site. In ZPEG241, the G-to-A mutation of the intron 6 generates a 21 nt shorter mutant of *PEX5L* mRNA. However, neither $Pex5p_{ZPEG241}$, 7 amino acid truncated form of Pex5pL, nor Pex5pL is detectable in ZPEG241 in the immunoblot with antibody to full-length Pex5pS (*5*). Interestingly, $Pex5p_{ZPEG241}$is identical to Pex5pM that is reported at mRNA level by RT–PCR using total RNA from CHO-K1 cells stably expressing GFP-SKL (*32*). $Pex5p_{ZPEG241}$ is dysfunctional in PTS2 import because of the defect in binding to Pex7p-PTS2 complexes, while Pex5pM is functional in PTS1 import. Currently, we and other group (*32*) are not able to detect the expression of endogenous Pex5pM, and the expression of *PEX5M* in CHO-K1 was <10% of total 29 cloned *PEX5* transcripts (data not shown) and 25% (*32*). Therefore, we conclude that Pex5pM does not play a pivotal role in peroxisome matrix protein import at least in CHO-K1 cells.

We earlier provided several lines of evidence that Pex5pL is exclusively involved in the PTS2 transport by directly binding to Pex7p carrying the cargo, PTS2-proteins (*5*, *18*). Two groups including ours demonstrated that the N-terminal part encompassing the primary sequence at positions 1–233 of Pex5pL is sufficient for PTS2-import (*19*, *33*). For the binding to Pex7p, 44 amino acid residues at 190-233 of Pex5pL are required (*19*). However, the residues at 190–223 are not sufficient, hence strongly suggesting that 10 amino acid sequence at 224–233 of Pex5pL, incidentally present in $Pex5p_{ZPEG241}$, is essential for the interaction of Pex5pL with Pex7p (*19*). In the present work, the N-terminal 7 amino acid residues at 216–222 of the Pex5pL-specific 37 amino acid insertion are also shown to be important for the Pex5pL binding to Pex7p. Taken theses results together, the entire region of the N-terminal part comprising 18 amino acids in the 37 amino acid insertion sequence is prerequisite for the binding of Pex5pL to Pex7p.

In ZPEG241 cells, Pex5pL expression is completely eliminated by the point mutation of 3′-acceptor splice site at 1 nt upstream of the exon 7 encoding Pex5pL-specific 37 amino acid insertion. Contrary to Pex5pL expression, mRNA for and protein of Pex5pS are expressed nearly at the same level in TkaEG2. Therefore, the expression level of Pex5pL and Pex5pS is more likely regulated in a mutually independent manner. The impaired expression of Pex5pL and apparently undetectable level of $Pex5p_{ZPEG241}$ in ZPEG241 are indeed a unique phenotype, opening a way to readily and further investigate the roles of Pex5pL under different physiological conditions devoid of endogenous Pex5pL. Moreover, in addition to Pex5pL* and Pex5pS*, the Pex5pL and Pex5pS are also expressed in CHO cells and human cells as verified in several cell lines. It is a very intriguing issue what is

the physiological consequence of such another type of Pex5p in these mammalian species.

Acknowledgements

We thank Y. Nanri for technical assistance, M. Nishi for preparing figures and the other members of our laboratory for discussion.

Funding

Science and Technology Agency of Japan, SORST and CREST grant (to Y.F.); Grants-in-Aid for Scientific Research (to Y.F.); The Ministry of Education, Culture, Sports, Science and Technology of Japan, The Global COE Program; Japan Foundation for Applied Enzymology, grant (to Y.F.).

Conflict of interest

None declared.

References

1. Fujiki, Y., Okumoto, K., Kinoshita, N., and Ghaedi, K. (2006) Lessons from peroxisome-deficient Chinese hamster ovary (CHO) cell mutants. *Biochim. Biophys. Acta-Mol. Cell Res.* **1763**, 1374–1381
2. Lazarow, P.B. and Fujiki, Y. (1985) Biogenesis of peroxisomes. *Annu. Rev. Cell Biol.* **1**, 489–530
3. Subramani, S., Koller, A., and Snyder, W.B. (2000) Import of peroxisomal matrix and membrane proteins. *Annu. Rev. Biochem.* **69**, 399–418
4. Otera, H., Okumoto, K., Tateishi, K., Ikoma, Y., Matsuda, E., Nishimura, M., Tsukamoto, T., Osumi, T., Ohashi, K., Higuchi, O., and Fujiki, Y. (1998) Peroxisome targeting signal type 1 (PTS1) receptor is involved in import of both PTS1 and PTS2: studies with *PEX5*-defective CHO cell mutants. *Mol. Cell. Biol.* **18**, 388–399
5. Otera, H., Harano, T., Honsho, M., Ghaedi, K., Mukai, S., Tanaka, A., Kawai, A., Shimizu, N., and Fujiki, Y. (2000) The mammalian peroxin Pex5pL, the longer isoform of the mobile PTS1-transporter, translocates Pex7p-PTS2 protein complex into peroxisomes via its initial docking site, Pex14p. *J. Biol. Chem.* **275**, 21703–21714
6. Matsumura, T., Otera, H., and Fujiki, Y. (2000) Disruption of interaction of the longer isoform of Pex5p, Pex5pL, with Pex7p abolishes the PTS2 protein import in mammals: study with a novel *PEX5*-impaired Chinese hamster ovary cell mutant. *J. Biol. Chem.* **275**, 21715–21721
7. Ghaedi, K. and Fujiki, Y. (2008) A new method for isolation of CHO cell mutants defective in peroxisome assembly, using ICR191 as a potent mutagenic agent. *Cell Biochem. Funct.* **26**, 684–691
8. Ghaedi, K., Kawai, A., Okumoto, K., Tamura, S., Shimozawa, N., Suzuki, Y., Kondo, N., and Fujiki, Y. (1999) Isolation and characterization of novel peroxisome biogenesis-defective Chinese hamster ovary cell mutants using green fluorescent protein. *Exp. Cell Res.* **248**, 489–497
9. Yanago, E., Hiromasa, T., Matsumura, T., Kinoshita, N., and Fujiki, Y. (2002) Isolation of Chinese hamster ovary cell *pex* mutants: two *PEX7*-defective mutants. *Biochem. Biophys. Res. Commun.* **293**, 225–230
10. Tsukamoto, T., Yokota, S., and Fujiki, Y. (1990) Isolation and characterization of Chinese hamster ovary cell mutants defective in assembly of peroxisomes. *J. Cell Biol.* **110**, 651–660
11. Tsukamoto, T., Miura, S., and Fujiki, Y. (1991) Restoration by a 35K membrane protein of peroxisome assembly in a peroxisome-deficient mammalian cell mutant. *Nature* **350**, 77–81
12. Okumoto, K., Shimozawa, N., Kawai, A., Tamura, S., Tsukamoto, T., Osumi, T., Moser, H., Wanders, R.J.A., Suzuki, Y., Kondo, N., and Fujiki, Y. (1998) *PEX12*, the pathogenic gene of group III Zellweger syndrome: cDNA cloning by functional complementation on a CHO cell mutant, patient analysis, and characterization of Pex12p. *Mol. Cell. Biol.* **18**, 4324–4336
13. Matsuzaki, T. and Fujiki, Y. (2008) The peroxisomal membrane-protein import receptor Pex3p is directly transported to peroxisomes by a novel Pex19p- and Pex16p-dependent pathway. *J. Cell Biol.* **183**, 1275–1286
14. Honsho, M., Yagita, Y., Kinoshita, N., and Fujiki, Y. (2008) Isolation and characterization of mutant animal cell line defective in alkyl-dihydroxyacetonephosphate synthase: localization and transport of plasmalogens to post-Golgi compartments. *Biochim. Biophys. Acta- Mol. Cell Res.* **1783**, 1857–1865
15. Shimizu, N., Itoh, R., Hirono, Y., Otera, H., Ghaedi, K., Tateishi, K., Tamura, S., Okumoto, K., Harano, T., Mukai, S., and Fujiki, Y. (1999) The peroxin Pex14p: cDNA cloning by functional complementation on a Chinese hamster ovary cell mutant, characterization, and functional analysis. *J. Biol. Chem.* **274**, 12593–12604
16. Miyata, N. and Fujiki, Y. (2005) Shuttling mechanism of peroxisome targeting signal type 1 receptor, Pex5: ATP-independent import and ATP-dependent export. *Mol. Cell. Biol.* **25**, 10822–10832
17. Honsho, M., Asaoku, S., and Fujiki, Y. (2010) Posttranslational regulation of fatty acyl-CoA reductase 1, Far1, controls ether glycerophospholipid synthesis. *J. Biol. Chem.* **285**, 8537–8542
18. Mukai, S. and Fujiki, Y. (2006) Molecular mechanisms of import of peroxisome-targeting signal type 2 (PTS2) proteins by PTS2 receptor Pex7p and PTS1 receptor Pex5pL. *J. Biol. Chem.* **281**, 37311–37320
19. Otera, H., Setoguchi, K., Hamasaki, M., Kumashiro, T., Shimizu, N., and Fujiki, Y. (2002) Peroxisomal targeting signal receptor Pex5p interacts with cargoes and import machinery components in a spatiotemporally differentiated manner: conserved Pex5p WXXXF/Y motifs are critical for matrix protein import. *Mol. Cell. Biol.* **22**, 1639–1655
20. Miyazawa, S., Osumi, T., Hashimoto, T., Ohno, K., Miura, S., and Fujiki, Y. (1989) Peroxisome targeting signal of rat liver acyl-coenzyme A oxidase resides at the carboxy terminus. *Mol. Cell. Biol.* **9**, 83–91
21. Okumoto, K., Bogaki, A., Tateishi, K., Tsukamoto, T., Osumi, T., Shimozawa, N., Suzuki, Y., Orii, T., and Fujiki, Y. (1997) Isolation and characterization of peroxisome-deficient Chinese hamster ovary cell mutants representing human complementation group III. *Exp. Cell Res.* **233**, 11–20
22. Ito, R., Huang, Y., Yao, C., Shimozawa, N., Suzuki, Y., Kondo, N., Imanaka, T., Usuda, N., and Ito, M. (2001) Temperature-sensitive phenotype of Chinese hamster ovary cells defective in PEX5 gene. *Biochem. Biophys. Res. Commun.* **288**, 321–327
23. Kemp, S., Wei, H.-M., Lu, J.-F., Braiterman, L.T., McGuinness, M.C., Moser, A.B., Watkins, P.A., and Smith, K.D. (1998) Gene redundancy and pharmacological gene therapy: implications for X-linked adrenoleukodystrophy. *Nat. Med.* **4**, 1261–1268
24. Mukai, S., Ghaedi, K., and Fujiki, Y. (2002) Intracellular localization, function, and dysfunction of

the peroxisome-targeting signal type 2 receptor, Pex7p, in mammalian cells. *J. Biol. Chem.* **277**, 9548–9561
25. Fujiki, Y. (1997) Molecular defects in genetic diseases of peroxisomes. *Biochim. Biophys. Acta* **1361**, 235–250
26. Subramani, S. (1997) *PEX* genes on the rise. *Nat. Genet.* **15**, 331–333
27. Rehling, P., Marzioch, M., Niesen, F., Wittke, E., Veenhuis, M., and Kunau, W.-H. (1996) The import receptor for the peroxisomal targeting signal 2 (PTS2) in *Saccharomyces cerevisiae* is encoded by the *PAS7* gene. *EMBO J.* **15**, 2901–2913
28. Zhang, J.W. and Lazarow, P.B. (1995) *PEB1* (*PAS7*) in *Saccharomyces cerevisiae* encodes a hydrophilic, intra-peroxisomal protein that is a member of the WD receptor family and is essential for the import of thiolase into peroxisomes. *J. Cell Biol.* **129**, 65–80
29. Braverman, N., Steel, G., Obie, C., Moser, A., Moser, H., Gould, S.J., and Valle, D. (1997) Human *PEX7* encodes the peroxisomal PTS2 receptor and is responsible for rhizomelic chondrodysplasia punctata. *Nat. Genet.* **15**, 369–376
30. Motley, A.M., Hettema, E.H., Hogenhout, E.M., Brites, P., ten Asbroek, A.L.M.A., Wijburg, F.A., Baas, F., Heijmans, H.S., Tabak, H.F., Wanders, R.J.A., and Distel, B. (1997) Rhizomelic chondrodysplasia punctata is a peroxisomal protein targeting disease caused by a non-functional PTS2 receptor. *Nat. Genet.* **15**, 377–380
31. Purdue, P.E., Zhang, J.W., Skoneczny, M., and Lazarow, P.B. (1997) Rhizomelic chondrodysplasia punctata is caused by deficiency of human *PEX7*, a homologue of the yeast PTS2 receptor. *Nat. Genet.* **15**, 381–384
32. Ito, R., Morita, M., Takahashi, N., Shimozawa, N., Usuda, N., Imanaka, T., and Ito, M. (2005) Identification of Pex5pM, and retarded maturation of 3-ketoacyl-CoA thiolase and acyl-CoA oxidase in CHO cells expressing mutant Pex5p isoforms. *J. Biochem.* **138**, 781–790
33. Dodt, G., Warren, D., Becker, E., Rehling, P., and Gould, S.J. (2001) Domain mapping of human PEX5 reveals functional and structural similarities to *Saccharomyces cerevisiae* Pex18p and Pex21p. *J. Biol. Chem.* **276**, 41769–41781